moment is reduced by the three-dimensional interactions from what it would be if the field were purely two-dimensional.

Further work has been initiated to extend the considerations to perturbations on cones. Because of the increase in complexity of the HSDT equations, it would seem that the Newtonian approximation should be applied at the outset for this case.

References

[1] Van Dyke, M. D., "A study of hypersonic small disturbance theory," NACA Rept. 1194 (1954).

[2] Hayes, W. and Probstein, R., *Hypersonic Flow Theory* (Academic Press, New York, 1959), Chap. 11.

[3] Cole, J. D., "Newtonian flow theory for slender bodies," J. Aeronaut. Sci. 24,448455 (1957).

[*] Guiraud, J. P., "Ecoulements hypersoniques infiniment voisins de l'ecoulement sur un diedre," Compt. Rend. 224, 2281–2284 (1957).

[5] Holt, M. and Yim, B., "Supersonic flow past finite double wedge wings of variable thickness," Parts I and II, Air Force Office of Scientific Research TN 60-431, 2 (1960).

[6] Malmuth, N., "Perturbations on hypersonic wedge flow," Ph. D. Thesis, California Institute of Technology (1962).

[7] Busemann, A., "Infinitesimal conical supersonic flow," NACA TM 1100 (**1947**).

[8] Lagerstrom, P., "Linearized theory of conical wings," NACA TN 1685 (1948).

Laminar, Transitional, and Turbulent Heat Transfer after a Sharp Convex Corner

Victor Zakkay,* Kaoru Toba,† and Ta-Jin Kuo‡

Polytechnic Institute of Brooklyn, Freeport, N. Y.

A flow model has been previously developed for treating the boundary-layer characteristics downstream of a surface discontinuity. The flow field in the neighborhood of the discontinuity or a sharp corner is divided into three regions: the flow upstream of the discontinuity which is obtained by standard techniques, that immediately downstream which is obtained by expanding both the supersonic and subsonic flow fields upstream of the discontinuity inviscidly around the corner, and that downstream of the discontinuity. The flow in the last region is represented by a viscous nonsimilar sublayer that starts at the discontinuity and by a viscous shear layer that has the profiles immediately downstream of the discontinuity as initial conditions. Based upon this flow model, analysis has been developed using the inner and outer expansion techniques. It is the purpose of this report to improve on the treatment of the laminar analysis and to extend the technique of application of this model to include turbulent and transitional flow downstream of the corner. Finally, the results are compared with some of the experimental data available in the literature. It is indicated that good agreement was obtained.

Nomenclature

c	$=$ const $= \rho\mu$
C_1	$=$ constant defined in Eq. (3a)
D	$=$ constant defined in Eq. (9)
$f_0(\eta), f_{1/2}(\eta),$	
$\quad f_{1/2\ 1/2}(\eta),$	
$\quad f_i(\eta)$	$=$ functions of η (see Ref. 2)
$g_0(\eta), g_1(\eta)$	$=$ functions of η (see Ref. 2)
h	$=$ enthalpy
H	$=$ total enthalpy
M	$=$ Mach number
Nu	$=$ Nusselt number
p	$=$ pressure
Pr	$=$ Prandtl number
q	$=$ amount of heat transferred at the wall per unit time and unit area
Re_s	$=$ Reynolds number defined by $\rho_{se}(H_{ei})^{1/2}R_0/\mu_{se}$
R_0	$=$ reference length
s	$= \int_0^x \rho_{ei}\mu_{ei}u_e dx$

u, U	$=$ velocity components x direction
v	$=$ velocity component in y direction
x, y	$=$ Cartesian coordinates
δ	$=$ thickness of shear layer (or boundary layer)
e	$=$ momentum thickness
$\varkappa$	$=$ coefficient of heat conduction
μ	$=$ coefficient of viscosity
ν	$=$ coefficient of kinematic viscosity
ρ	$=$ density
σ	$=$ measure of vorticity gradient defined in Eq. (3)
τ	$=$ variable defined in Eq. (3)
Φ	$=$ measure of curvature of enthalpy profile defined in Eq. (3)
ψ	$=$ stream function
ω	$=$ measure of vorticity defined in Eq. (3)
Ω	$=$ measure of slope in enthalpy profile defined in Eq. (3)

Subscripts

ei	$=$ condition external to shear layer
se	$=$ stagnation condition after normal shock
$*$	$=$ reference state

Introduction

IN many practical problems in hypersonic flight, bodies having surface discontinuities or regions with rapid variation of curvature are used. Typical bodies of such type are, for example, cone-cylinder combinations.

A sublayer model for the boundary-layer characteristics downstream of the corner was first introduced by Sternberg.[1]
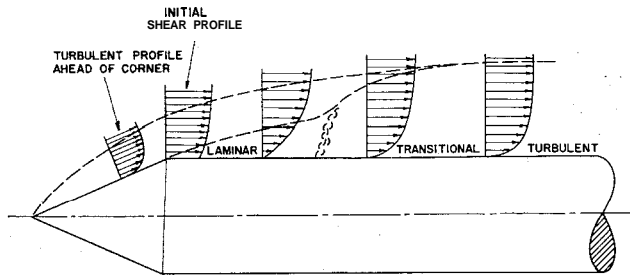
Fig. 1 Scheme for analyzing corner, turbulent ahead of corner.

In Sternberg's paper, the predicted boundary-layer characteristics are compared with measurements of the recovery factor. At a later date, independently, Zakkay and Tani[2] reintroduced the same model and presented a detailed method for evaluating the development of shear layer and sublayer as well as the heat-transfer rate when the oncoming boundary layer is laminar. These analyses were made by using an expansion technique similar to that used by Gortler. In the present work, the forementioned technique is extended to include both transitional and turbulent boundary layers. Again in this case, the method chosen for analyzing the boundary-layer characteristics is based on the model introduced in Ref. 1.

According to the sublayer model, the flow field of interest may be divided into two layers, an inner nonsimilar layer starting at the corner and an outer shear layer. The initial conditions for the shear layer are obtained by the inviscid and adiabatic expansion of the boundary-layer profiles ahead of the corner. The new viscous layer is shown in Fig. 1 and will be referred to as sublayer since it underlies the outer shear layer. Distinction should be made between the proposed sublayer and the one usually associated with turbulent flow.

This flow model presupposes that the initial velocity profile of the shear layer is very steep. In effect, the flow field downstream of the corner will be considered the same as that which would exist over a flat plate, with oncoming viscous flow having shear and shear gradient. Consequently, the corner itself is treated as a singularity similar to the leading edge of a flat plate. Hence, the problem is similar to the one treated by Li[3] and Glauert.[4] However, in this case, the analysis uses the experimental pressure distribution and will not be concerned with the higher-order effects such as the induced pressure gradient.

When the boundary-layer flow is fully turbulent up to the corner, the sublayer model is expected to become more effective since the velocity profile is steeper than the one obtained for laminar flow.

Mathematical treatment, however, is not developed rigorously because of the new unknowns, i.e., Reynolds stress and turbulent heat flux. Moreover, according to the equivalence of the flow field to a flow over a flat plate placed in a turbulent oncoming flow, the flow represented by the sublayer may be laminar close to the corner and may undergo the transition to turbulence somewhere downstream. Four independent sets of experimental data presented show that the observed heat-transfer rate has such a trend. Taking into account such a phenomenon, the sublayer plus simple mass flow consideration gives good results of heat-transfer rate near the

corner and somewhat downstream of the corner where the state of affairs becomes asymptotic.

Laminar Flow

A detailed analysis of the laminar treatment of the boundary-layer characteristics after the corner has been presented in Ref. 2. The boundary layer has been analyzed in two parts; a sublayer starting at the corner and analyzed by utilizing a series expansion for nonsimilar solutions as suggested by Görtler,[5] and a viscous shear layer at the outer edge which utilizes the same type of series solutions and has the inviscid profiles immediately downstream of the discontinuity as initial conditions. From the boundary-layer solution, an expression for obtaining the heat transfer downstream of the corner has been given.

In Ref. 2, the analysis has been carried out without utilizing the Crocco relationship. However, it is indicated that, for the case where the pressure gradient is small after the corner, one can expect the Crocco relation between the velocity and the enthalpy to hold.

For this case, the solutions for the velocity and enthalpy profiles are indicated below[2]:

$$u = u_e \left\{ f_0'(\eta) + \frac{(2s)^{1/2}}{u_e \delta_1} \omega f_{1/2}'(\eta) + \frac{2s}{u_e^2 \delta_1^2} [\omega^2 f'_{1/2\,1/2}(\eta) + \sigma f_1'(\eta)] + O(s^{3/2}) \right\} \quad (1)$$

$$H = h_w + (h_0 - h_w)g_0(\eta) + \frac{(2s)^{1/2}}{u_e \delta_1} \{(h_0 - h_w)\omega f_{1/2}'(\eta) + [h_0\Omega - (h_0 - h_w)\omega]g_{1/2}(\eta)\} + \frac{2s}{u_e^2 \delta_1^2} [(h_0 - h_w)\omega^2 f'_{1/21/2}(\eta) + \sigma(h_0 - h_w)g_1(\eta)] + O(s^{2/3})$$

(2)

where

$$\tau = \frac{1}{\delta_1} \int_0^y \rho dy \qquad \delta_1 = \left(\int_0^\delta \rho dy\right)_{x=0}$$

$$s = \int_0^x \rho_{ei} \mu_{ei} u_e dx$$

The function $f_0'(\eta)$ pertains to the Blasius part of the solution of the flat plate boundary-layer equation; $f_{1/2}'(\eta)$, $f'_{1/2\,1/2}(\eta)$, and $f_1'(\eta)$ belong to the Gortler series and are due to the nonsimilar behavior of the profile. The quantity u_e is a reference velocity that is determined from the matching condition of the sublayer and shear layer and is equal to u_0 in Eq. (3). ω and σ are terms that define the shape of the shear velocity profile as expressed in Eq. (3). The transformation between the coordinate for the sublayer η to the coordinate of the shear layer is given by

$$\eta = [\delta_1 u_e/(2s)^{1/2}]\tau$$

The term in the energy equation $g_0(\eta)$ pertains to the zero-order solution and is shown to be equal to $f_0'(\eta)$, whereas $g_{1/2}(\eta)$, $g(\eta)$ pertain to the higher-order solution because of the nonsimilarity in the profiles. Ω and Φ are terms that define the shape of the shear enthalpy profile as expressed in Eq. (3). The details of this analysis may be obtained from Ref. 2.

The shear profiles obtained after the expansion at the corner have been expressed as

$$U_0(\tau) = u_0(1 + \omega\tau + \sigma\tau^2 + \ldots)$$

$$H_0(\tau) = h_0(1 + \Omega\tau + \Phi\tau^2 + \ldots)$$

(3)

Table 1   Solution to higher-order equations

$f_0''(0)$	0 4696	$g_0'(0)$	0 4696
$f_{1/2}''(0)$	0.7950	$g_{1/2}'(0)$	0 4572
$f_1''(0)$	1.1564	$g_1'(0)$	1 1564[a]
$f_{1/2\,1/2}''(0)$	0.1576"	...	..

[a] Far $p_1 = 0$.

where the two profiles may be related by the Crocco relation through the following equations:

$$C_1 u_0 + h_w = h_0$$
$$C_1 u_0 \omega = h_0 \Omega \qquad (3a)$$
$$C_1 u_0 \sigma = h_0 \Phi$$

where C_1 is an arbitrary constant.

The details of the derivation and the tabulation of the functions $f_0(\eta), f_{1/2}(\eta), \ldots, g_1(\eta)$ will be presented in a subsequent report. The values of derivatives of direct interest are given in Table 1 where p_1 indicates axial pressure gradient.

The heat-transfer rate at the wall can be expressed in a nondimensional form as

$$\frac{Nu}{Re_s^{1/2}} = \frac{q C_{pse} R_0}{\varkappa_{se}(H_{ei} - h_w)} \frac{1}{Re_s^{1/2}} \qquad (4a)$$

where

$$q = \frac{\varkappa}{C_p}\left(\frac{\partial H}{\partial \eta}\frac{\partial \eta}{\partial y}\right)_{y=0} = \frac{\varkappa}{C_p \mu_w}\frac{u_0 \rho_w \mu_w}{(2s)^{1/2}}\left(\frac{\partial H}{\partial \eta}\right)_{\eta=0} \qquad (4b)$$

where q is the amount of heat transferred per unit time area, $Re, = \rho_{se}(H_{ei})^{1/2}R_0/\mu_{se}$ and the suffix se refer to the conditions after a normal shock of the undisturbed flow.

The experiments for a sharp cone-cylinder as well as for a blunt cone are described in Ref. 2. The pertinent flow quantities for the 20° sharp cone-cylinder arc stagnation pressure, 600 psia; stagnation temperature, 1800°R; wall-to-stagnation temperature ratio, 0.313; $Re,$, 3 × 10⁴; freestream Mach number, 8; and Mach number outside the boundary layer, 4.25 before the corner and 6.63 after the corner. Using the experimental data, q is obtained from Eq. (2). Then Eqs. (4) finally result in

$$(Nu/Re_s^{1/2}) \cdot 10^3 = (8.619/x^{1/2}) + 6.6 + 1.14 x^{1/2} + \ldots \qquad (5)$$

where p_1 is assumed zero and x is measured in inches. The results are plotted in Fig. 2. Also included for comparison is the flat plate solution corresponding to the uniform flow at the edge of the outer shear layer. The ratio of the fourth term in Eq. (5), which is omitted, to the third term is $O(x^{1/2}/10)$ and is also proportional to $Re_s^{-1/2}$. For the present value of $Re,$, the fourth term becomes of appreciable magnitude at $x = 100$ in. Also included is Van Driest's flat plate solution n which the assumptions of Prandtl number equal to unity and $\rho\mu = C$ are relaxed. Correction to these effects can be made easily. However, as is evident from Fig. 2, present results show satisfactory agreement with the experiment for most engineering purposes. In order to further substantiate the applicability of this theory, the results of the analysis are compared with the experimental results of Ref. 6. The pertinent flow quantities for the 15° sharp cone-cylinder arc stagnation pressure, 139 psia; stagnation temperature, 710°R; wall-to-stagnation temperature ratio, refer to Fig. 3; Re_s, 3.74 × 10⁵; freestream Mach number, 5; and Mach number outside the boundary layer, 3.8 before the corner and 5.12 after the corner. From these data, Eq. (4) finally results in

$$(Nu/Re_s^{1/2}) \cdot 10^3 = (2.3295/x^{1/2}) + 1.693 + \ldots \qquad (6)$$

where p_1 is assumed zero, x is measured in inches, and the initial profiles are linearized. The results arc plotted in Fig. 3. Again, the results show satisfactory agreement with the experiment. The experimental data have been replotted in terms of the Nusselt number and Reynolds number defined in this paper.

Turbulent Flow

For turbulent flows, mathematical treatment becomes increasingly difficult. Nevertheless, it will be shown here
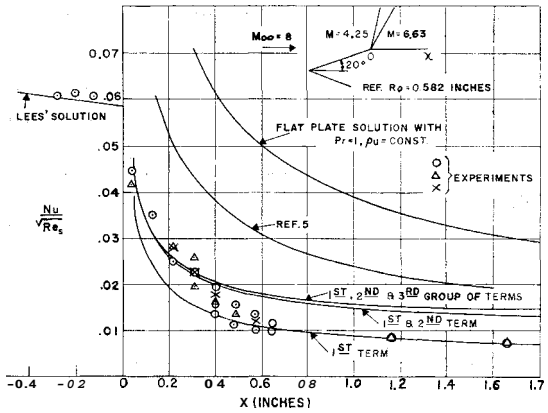
Fig. 2 Laminar heat-transfer distribution for a 20" sharp cone-cylinder.

that the sublayer model coupled with some simple physical arguments results in a sufficiently accurate prediction of the heat-transfer rate. For this case the boundary layer ahead of the corner will be turbulent. Two cases will be considered here. The first case will be for the condition where the boundary layer is artificially tripped, and the second case will be for the condition where the freestream Reynolds number is sufficiently high for a turbulent boundary layer to be established before the corner.

A. Method of Analyzing Boundary Layer Upstream of Corner

In order to insure that the boundary layer ahead of the corner was turbulent, the heat-transfer rate in each case was calculated using standard turbulent boundary-layer analysis. The velocity and enthalpy profiles ahead of the corner were calculated by using the tabulations of Ref. 7 for a (one-seventh) power law for the velocity profile. The heat transfer to the cone has been calculated by the flat rate reference enthalpy method.[8] For a not so slender cone in a supersonic flow with attached bow shock wave, Van Driest's law[9] may
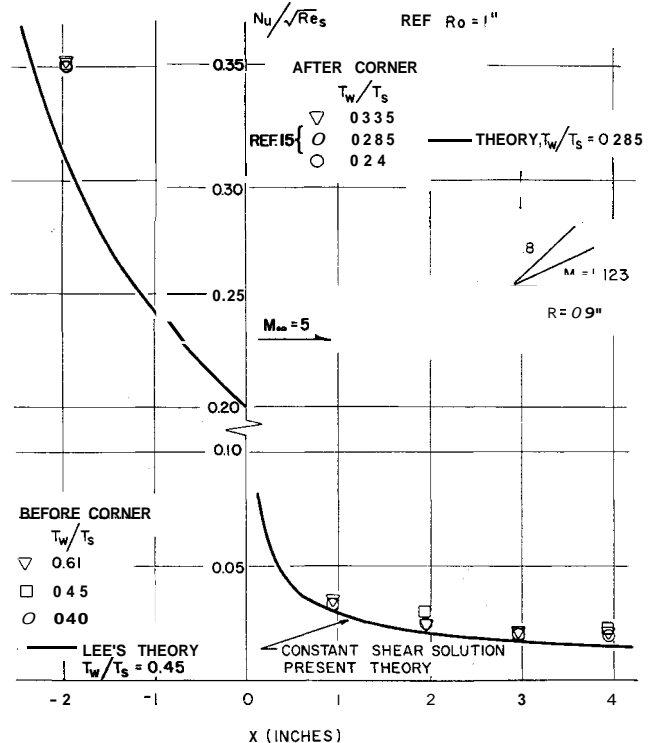
Fig. 3 Laminar heat-transfer distribution for a 15° sharp cone-cylinder.

be applied to calculate the skin friction and, hence, the heat transfer. According to this rule, the cone skin friction is evaluated with one-half the Reynolds number for flat plate with the same freestream temperature ratio. The temperature profile follows from the Crocco relation with corrections for the Prandtl number. In each case the momentum thickness ahead of the corner has been calculated. It is also indicated here that when $Re_\theta = 600$ to 700, a turbulent boundary layer prevails ahead of the corner on the conical portion of the model.

B. Expansion around the Corner

In this step the viscosity is neglected. The velocity and stagnation enthalpy profiles are expanded isentropically around the corner. In this manner a velocity profile having a nonzero value at the wall and a corresponding stretched-out stagnation enthalpy profile are obtained downstream of the corner. This scheme has been proposed in Ref. 1 and has been used successfully in Ref. 2. Reference 1 points out that the high acceleration present at the corner has an effect of reducing the turbulence level in the boundary layer. This is similar to the reduction in turbulence level obtained by the contraction section of a wind tunnel. Morkovin[10] has made a detailed study of the effect of a sudden expansion on a turbulent boundary layer. In this study, the expansion was produced on a flat plate by means of a wedge. Detailed profile measurements of pitot pressure and velocity fluctuations before and after the expansion were made. The results indicated that the assumption of isentropy in the boundary layer during the expansion is valid. The measurements of the velocity fluctuations in percent of local mean velocity before and after the corner indicated a decrease close to the wall and an increase toward the outside part of the boundary layer. Therefore, the results of Refs. 1, 2, and 10 justify the inviscid expansion assumed in this part of the paper. In each case the momentum thickness is calculated from the density and velocity profiles obtained after the expansion with the following equation:

$$\theta = \int_0^\delta \frac{\rho u}{\rho_e U_e} \left(1 - \frac{u}{U_e}\right) d\eta \qquad (7)$$

C. Analysis of Boundary Layer Downstream of Corner

Reference 1 has indicated that the effect of a rapid expansion around the corner enables the growth of a new laminar boundary layer starting at the beginning of the cylinder. It is also believed1 that the extent of the new laminar boundary layer, and the transition to turbulent flow, is controlled by the turbulence level present in the shear layers after the expansion. Detailed calculations have been carried out in Ref. 1 in order to support the foregoing statement.

Therefore, since the initial part of the boundary sublayer after the corner is laminar, analysis developed for the laminar sublayer is also applicable here. The shear profiles for the laminar sublayer will be the ones obtained from the inviscid expansion of the turbulent profiles obtained ahead of the corner. In this it is assumed that the fluctuations in the shear layer have a negligible effect on the formulation of the laminar sublayer.

Next, consideration will be given to the development of the asymptotic flow downstream of the corner. It is well known that turbulent boundary-layer profiles at high Reynolds number preserve their self-similar character over the greater part of the flow provided there is no pressure gradient.[11, 12] For the present case, despite the negligibly small pressure gradient, self-similarity may not be expected within at least some distance downstream of the corner. This is because of the transient state immediately after the rapid expansion. The flow must adjust itself for some distance

until it approaches the asymptotic state where the self-similar character prevails again. This state may be reached roughly when the sublayer swallows up the mass flow contained in the initial velocity profile immediately after the corner. Thus, the complicated transient phenomenon of the over-all viscous layer is now replaced by the changing proportion of the sublayer and the shear layer; the latter is absorbed in the former. In this argument, a simplifying assumption has been made that the velocity profile of the outer shear layer does not change appreciably for the range considered. In other words, additional mass entrained within the shear layer and the displacement effect of the sublayer on the shear layer are neglected. Further simplifications may be made by approximating linearly the average initial profiles immediately after the corner. The sublayer will be first assumed fully turbulent from the corner. Since it is assumed to preserve its self-similar character all the way (one-seventh), power law is adopted for the velocity profile. Correspondingly, the heat-transfer rate can be calculated with the flat plate equations. The proper outer edge conditions correspond to those of the initial profiles obtained right after expansion. These outer edge conditions will provide the asymptotic solution. Having now established the turbulent asymptotic solution to the problem at some distance away from the corner and also having established the laminar region immediately downstream of the corner, it is now necessary to connect the two solutions. In this, a study of transition is necessary in order to obtain the complete solution.

Classically, transition is known to be influenced by a number of factors and cannot be given theoretically by any single parameter. Reference 1 has outlined a procedure for estimating the extent of laminar sublayer through a calculation of an axial turbulence parameter. However, in the past, the Reynolds number based on the momentum thickness has been used successfully to estimate the transition point independent of other factors. These observations have been based on experimental results and have been shown to be applicable for a wide variety of conditions. For instance, transition is observed to occur on the front portion of a hemisphere at an Re_θ of $300 \rightarrow 400$ whereas on the conical portion of a blunt body at an Re_6 of 700. Some recent data indicate that transition occurs on a flat plate at an Re_θ of 1300 1400. Therefore, as a first approximation, the same point of view will be taken here in order to get an idea where transition occurs.

It now remains to define the momentum thickness. Two different approaches may be taken. The first is to base the momentum thickness on the new laminar boundary layer alone, starting at the beginning of the cylinder and excluding the shear layer (suggestion made in Ref. 1), whereas in the other case, to base the momentum thickness on the over-all sublayer and shear layer. The reason for calculating the second Re_θ is to introduce some history into the new laminar boundary layer. Both Re_θ's will be calculated from all the cases.

The transitional region is analyzed following Refs. 13 and 14. Use is made of the same simplifying assumption that the profiles of the outer shear layer do not change appreciably for the range considered. The growth of the sublayer in the transformed plane is determined by solving the momentum equation using the empirical skin-friction expression in terms of $Re_{\theta*} = \nu_{e*}/U_{e*}\theta_*$:

$$d\theta_*/dx = C_{f*}/2 \qquad (8)$$

$$c_{f*} = \mu_*(\partial u_*/\partial y_*)\big|_{y_*=0}\, \rho_* u_e{}^2/2 =$$
$$0.0261\, Re_{\theta*}{}^{-1/4} - D Re_{\theta*}{}^{-2} \qquad (9)$$

Correspondingly, the thickness of the transitional sublayer is determined by the following relation:

$$\left(\frac{\delta_*}{\theta_*}\right)_{trans} = \left(\frac{\delta_*}{\theta_*}\right)_{turb} - \frac{G}{x}\left(\frac{\delta_*}{\theta_*}\right)_{lam} \qquad (10)$$

where the constants D and G are obtained by matching c_{f_*} and $(\delta_*/\theta_*)_{trans}$ with those of the laminar flow at the assumed transition point. Equation (8) is integrated numerically, yielding the distribution of the momentum thickness. From the local thickness of the sublayer and from the initial profiles of the outer shear layer, the local outer edge conditions of the sublayer are determined. From Eq. (9) the local skin friction and, hence, the local heat-transfer rate are obtained.

Discussion of Theoretical and Experimental Results

In order to demonstrate the various theoretical aspects discussed in the previous section, four experimental results are presented below.

Case 1

For this case the stagnation pressure is 600 psia; the stagnation temperature, 1700°R; wall-to-stagnation temperature ratio, 0.294; $Re_s = (\rho_s h_s^{1/2} R_0/\mu_s)(R_0 = 0.582$ in.), 4.94×10^4; freestream Mach number, 8; and the Mach number outside the boundary layer is 1.70 before the corner and 2.67 after the corner.

The foregoing test was conducted at the hypersonic facility of the Polytechnic Institute of Brooklyn. The body consists of a spherically capped 24° half angle cone-cylinder with a bluntness ratio of $R_0/r = 0.317$ (Fig. 4a). The laminar boundary-layer study over this body has been presented in Ref. 2. Experimental laminar heat-transfer results, as well as comparison with theory before and after the corner, were also included in Ref. 2. In order to make the boundary layer turbulent ahead of the corner, trips were placed at the nose portion of the model in order to induce transition. The pressure distribution over the model was measured with the trips and indicated that there was no change from the one obtained without the trips. Therefore, in these analyses the pressure distribution presented in Ref. 2 was used in calculating the heat transfer before and after the corner. The heat-transfer measurements are presented in Fig. 4a in the form of $Nu/(Re_s)^{1/2}$ vs x in inches. In order to insure that the boundary layer before the corner was turbulent, standard heat-transfer analysis was used to predict the heat transfer before the corner. The boundary-layer profiles ahead of the corner have been calculated with the aid of Refs. 7 and 9 and are presented in Fig. 4b. The Reynolds number based on the momentum thickness calculated for the profiles is $Re_\theta = 208$. The profiles obtained after the inviscid expansion around the corner are presented in Fig. 4c. The Reynolds number based on the momentum thickness after the expansion is 143. The heat transfer after the corner was calculated with the aid of the laminar boundary-layer equations (2) and (4) using the turbulent shear profiles presented in Fig. 4c. The results are presented in Fig. 4a, and it is clearly seen that the experimental data are well represented by the theory presented here. On the same figure, the turbulent solution for the heat transfer for the asymptotic state is also presented for verifying that the boundary layer obtained after the expansion is laminar. It is expected that this new laminar boundary layer will prevail for quite a distance downstream of the corner. No transition was observed in this case.

Case 2

In this case the stagnation pressure was 57.3 psia: the stagnation temperature, 660°R; wall-to-stagnation temperature ratio, 0.924; Re_s, 5.13×10^5; freestream Mach number, 3.04; and the Mach number outside the boundary layer was 1.88 before the corner and 2.39 after the corner.

The results of these tests have been taken from Ref. 6. The body tested consisted of a spherically capped 15° half

angle cone with a bluntness ratio of $R_0/r = 0.6$ (Fig. 5).

For the test conditions just presented, the Reynolds number was sufficiently high so that a turbulent boundary layer was well established ahead of the corner. In order to substantiate this, the turbulent heat transfer has been calculated ahead of the corner and is presented in Fig. 5 with the measurements. It is clearly seen that the experimental results are well presented by the turbulent solution. Figure 6a presents the boundary-layer profiles before the corner. In this case, Re_θ was calculated to be 750. The shear layer profiles obtained after the inviscid expansion around the corner are presented in Fig. 6b. For this condition, Re_θ was calculated to be 770.

Since a laminar boundary layer does prevail after the discontinuity, the heat transfer has been calculated according to Ref. 2 and is presented in Fig. 5. On the same figure, the asymptotic solution of the turbulent boundary layer is also presented. It is clearly indicated that transition occurs at $x = 0.8$ in. In this case, the Re_θ based on the sublayer alone was calculated to be 200, whereas an Re_θ of 1130 was
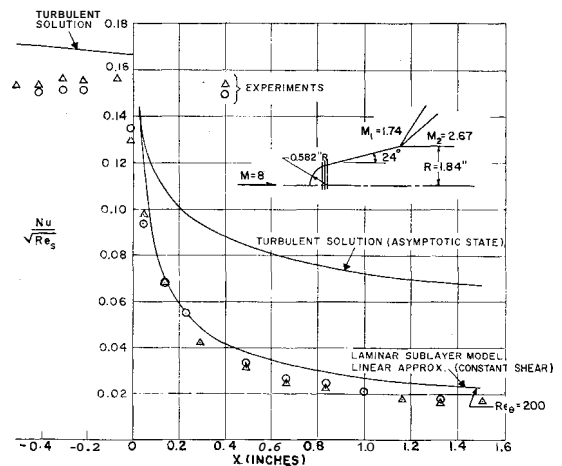
Fig. 4a   Heat-transfer distribution for a 24° blunted cone-cylinder.
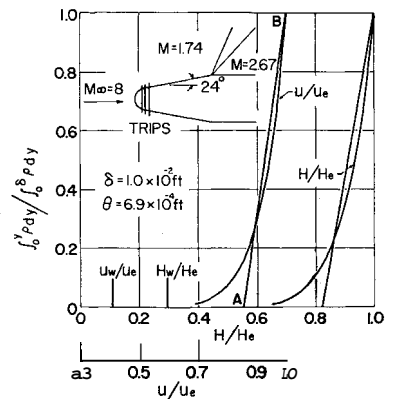
Fig. 4b   Turbulent boundary-layer profiles before expansion for a 24° blunted cone-cylinder.
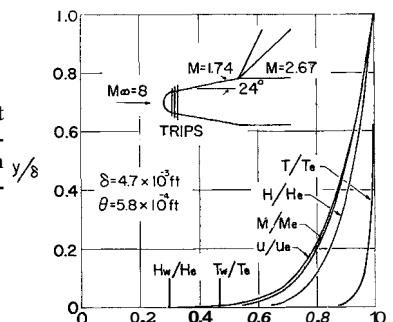
Fig. 4c   Turbulent boundary-layer profiles after expansion for a 24° blunted cone-cylinder.

calculated for the over-all sublayer and shear layer. With this, the transitional heat transfer was calculated with the aid of Eqs. (9) and (10) and is included in Fig. 5.

The previous experiment and the considerations presented in this paper bear out well that a laminar sublayer is followed by a second transition to turbulent flow.

Case 3

Here the stagnation pressure was 139 psia; the stagnation temperature, 710°R; wall-to-stagnation temperature ratio, 0.47; $Re_,,$ 3.73 × 10^5; freestream Mach number, 5.0; and the Mach number outside the boundary layer, 3.8 before the corner and 5.12 after the corner.

The results of these tests have been taken from Ref. 15. The body consisted of a 15" half angle sharp cone followed by a cylindrical afterbody 1.8 in. in diameter. The laminar results for this configuration have been presented in the laminar portion of this paper. In order to obtain a turbulent boundary layer, trips were placed on the conical portion of the body. The results of the heat-transfer measurements are presented in Fig. 7 in terms of the symbols used in this report. The Reynolds number based on the turbulent momentum thickness ahead of the corner was calculated to be 1370, whereas the one calculated after the expansion was 1530. The analysis for the laminar calculations as well as for the turbulent asymptotic solution are included in Fig. 7. Therefore, the boundary layer is closely approximated by the asymptotic turbulent solution. These considerations are clearly seen from the theoretical predictions included in Fig. 7. The experimental results are much higher than the
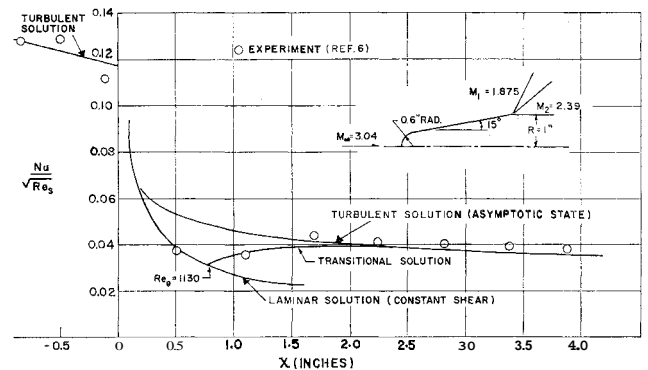

Fig. 6 Heat-transfer distribution for a 15° blunted cone-cylinder.

laminar predictions and are closer to the turbulent asymptotic solution.

Case 4

In order to get a further understanding of the transitional point, the results of Ref. 1 are included in the following: stagnation pressure, 27.1 psia; stagnation temperature, 535° R; wall-to-stagnation temperature ratio, adiabatic wall; $Re_,,$ 5.352 × 10^5; freestream Mach number, 3.02; and the Mach number outside the boundary layer, 1.89 before the corner and 3.13 after the corner.

The body considered in the foregoing test consisted of a 29° half angle sharp cone. The adiabatic wall temperature was measured before and after the corner for both laminar as well as turbulent conditions ahead of the corner. For the case where a laminar region prevailed ahead of the corner, Re_θ is calculated to be 540. Inviscid profiles after the corner were also obtained, and the corresponding Re_θ calculated for these profiles was 460. It is indicated in Ref. 1 that transition for this case was observed to occur at a distance of 20 cm downstream of the shoulder. Since for this condition the heat transfer is zero, the growth of the momentum thickness of the over-all layer downstream of the corner is calculated from the distribution of the skin-friction coefficient according to Eq. (8). The latter quantity, in turn, is calculated from Eq. (1). A value of Re_θ equal to 1200 was obtained from the analysis at the observed station of transition. The data of Ref. 1 indicate an Re_θ of about 1000 when the momentum thickness is based on the laminar sublayer alone.

For the case where the boundary layer was turbulent ahead of the corner, the value of Re_θ calculated before and after the corner is 1200 and 800, respectively. The portion where transition was observed for this condition was at 3 cm downstream of the shoulder. The Re_θ based on the total boundary layer calculated at the point of transition was equal to 1100, whereas an Re_θ of 340 was obtained for the laminar sublayer alone. It is interesting to observe here that the Re_θ based on the over-all boundary layer is the same and has the same value for both the laminar and the turbulent case.

Conclusions

A flow model has been adopted for treating the boundary layer downstream of a sharp corner. The analysis based on this model for a laminar flow was presented in Ref. 2. Improvements are made herein whereby a unified treatment of velocity and thermal profiles with the Crocco relation as the limiting case of zero pressure gradient thus are amenable to the calculation of the higher-order solution including the pressure gradient.

An extension of this flow model to conditions where the boundary layer ahead of the corner is turbulent is also included. These results were compared with some of the experimental results available in the literature.
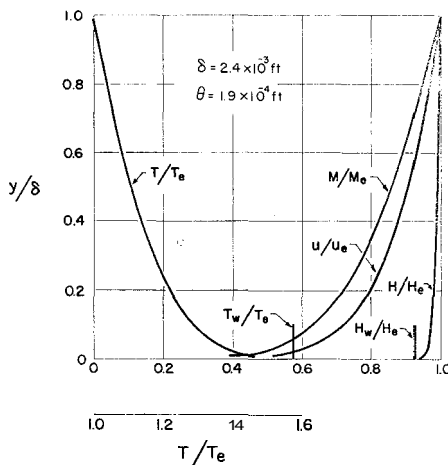

Fig. 5a Turbulent boundary-layer profiles before expansion for a 15° blunted cone-cylinder.
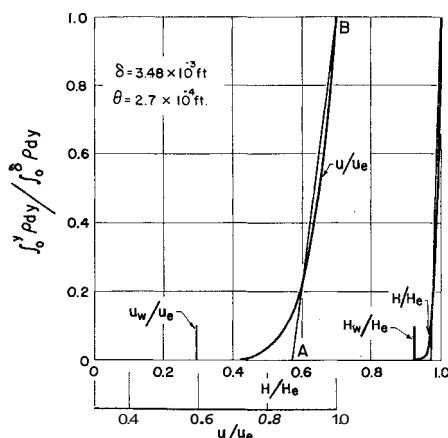

Fig. 5b Turbulent boundary-layer profiles after expansion for a 15° blunted cone-cylinder.
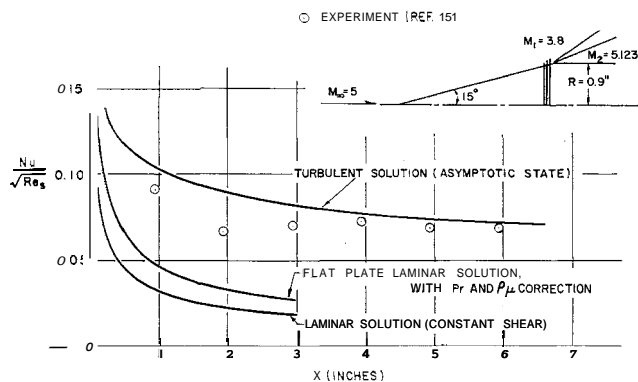
Fig. 7   Heat-transfer distribution for a 15" sharp cone-cylinder.

The results also reaffirmed the considerations presented by Sternberg that a new laminar boundary layer does start at the discontinuity. This boundary layer will prevail for a distance, and a second transition to turbulent will subsequently occur.

It is indicated here that, for the range of test conditions observed, if Re_s before the discontinuity is of the order of $600 \rightarrow 700$, then a turbulent boundary layer exists ahead of the discontinuity. From the results, the second transition to turbulent occurs at an Re_θ of $200 \rightarrow 300$ when the momentum thickness is based on the sublayer alone. These values correspond to an Re_s of $1100 \rightarrow 1300$ when based on the overall sublayer and shear layer. For the case when Re_θ (based on the initial momentum thickness) is larger than 1400, the heat transfer is predominantly turbulent for the range of experiments presented here. The results in this paper are not conclusive for the point when transition occurs, and additional data are necessary.

The heat-transfer analysis indicates also that the effect of shear on the development of the turbulent boundary layer after the discontinuity is of much less significance than for the laminar case.

References

[1] Sternberg, J., "The transition from a turbulent to a laminar boundary layer," Ballistic Research Lab. Rept. 906 (May 1964).

[2] Zakkay, V. and Tani, T., "Theoretical and experimental investigation of the laminar heat transfer downstream of a sharp corner," Polytechnic Institute of Brooklyn, PIBAL Rept. 708, Air Force Office of Scientific Research, AFOSR 1640 (October 1961); also Fourth U. S. National Congress of Applied Mechanics, Univ. of California, Berkeley, Calif. (June 18–21, 1962).

[3] Li, T. Y., "Effects of free-stream vorticity on the behavior of a viscous boundary layer," J. Aeronaut. Sci. 23, 1128–1129 (1956).

[4] Glauert, M. B., "The boundary layer in simple shear flow past a flat plate," J. Aeronaut. Sci. 24, 848–849 (1957).

[5] Gortler, H., "A new series for the calculation of steady laminar boundary layer flows," J. Math. Mech. 6, (1957).

[6] Inouye, M. and Sisk, J. B., "Wind-tunnel measurements at Mach numbers from 3 to 5 of pressure and turbulent heat transfer on a blunt cone-cylinder with flared afterbody," NASA TMX-654 (July 1962); confidential, Figs. 4 and 7 declassified February 12, 1963, title unclassified.

[7] Persh, J. and Lee, R., "Tabulation of compressible turbulent boundary layer parameters," Naval Ordnance Test Station NAVORD Rept. 4282 (1956).

[8] Eckert, E. R. G., "[Engineering relations for friction and heat transfer to surfaces in high velocity flow," J. Aeronaut. Sci. 22, 585–587 (1955).

[9] Van Driest, E. R., "Turbulent boundary layer on a cone in a supersonic flow at zero angle of attack," J. Aeronaut. Sci. 19, 55–57 (1952).

[10] Morkovin, M. V., "Effects of high acceleration on a turbulent supersonic shear layer," Proceedings of the 1966 Heat Transfer and Fluid Mechanics Institute (Stanford University Press, Stanford, Calif.).

[11] Lin, C. C. (ed.), Turbulent Flows and Heat Transfer (Princeton University Press, N. J., 1959), Vol. 5.

[12] Townsend, A. A., The Structure of Turbulent Shear Flow (Cambridge University Press, New York, 1956).

[13] Persh, J., "A method for calculating the boundary-layer development in the region of transition from laminar to turbulent flow," Naval Ordnance Test Station NAVORD Rept. 4438 (1957).

[14] Zakkay, V. and Callahan, C. J., "Laminar, transitional, and turbulent heat transfer to a cone-cylinder-flare body at Mach 8.0," Polytechnic Institute of Brooklyn, PIBAL Rept. 737, Air Force Office of Scientific Research AFOSR 2359 (February 1962); also J. Aerospace Sci. 29, 1403–1420 (1962).

[15] Schaefer, J. W. and Ferguson, H., "Investigation of separation and the associated heat transfer and pressure distribution on cone-cylinder-flare configurations at Mach 5," ARS Space Flight Report to the Nation, New York (October 9–15, 1961).